ChemComm

COMMUNICATION

View Article Online
View Journal | View Issue

A near-infrared-emitting fluorescent probe for monitoring mitochondrial pH†

Cite this: *Chem. Commun.*, 2014, **50**, 7184

Received 23rd February 2014,
Accepted 9th May 2014

DOI: 10.1039/c4cc01390e

www.rsc.org/chemcomm

Ping Li, Haibin Xiao, Yinfang Cheng, Wen Zhang, Fang Huang, Wei Zhang, Hui Wang and Bo Tang*

We demonstrate a new small molecule fluorescent probe, possessing near-infrared (NIR) emission and an unusually large Stokes shift. It can be readily taken up by live cells and mitochondria, and track subtle pH changes with effectively reduced biological background fluorescence and improved measurement accuracy.

Mitochondria are the double-membrane-bound subcellular organelles providing enormous metabolic functions,[1–4] such as producing much of the cellular energy, regulating the cellular redox state, generating most of the cellular reactive oxygen species (ROS),[5–7] and initiating cellular apoptosis.[8,9] The specific pH values of mitochondria influence directly all biochemical processes. So this parameter has to be severely controlled within a narrow range, and aberrations of the normal pH homeostasis may lead to mitochondrial dysfunction. Accurate and sensitive measurements of mitochondrial pH (pH_{mit}) dynamics in living cells are therefore crucial to the understanding of mitochondrial biology. However, despite previous extensive investigations focussing on mitochondrial biology, a great variety of their fundamental cellular functions still remain elusive, which is hampered severely by the shortage of ideal approaches for tracking mitochondrial biological events, including pH changes.

It is now generally accepted that organic fluorescent probes are some of the cornerstones of modern bioanalysis and real-time bioimaging technologies.[10–12] They offer excellent sensitivity and high spatial resolution while minimally perturbing the live cells and organisms. In particular, near-infrared (NIR) emission fluorescent probes are able to dramatically reduce influence of biological background fluorescence, which has grown into an important tool in widespread exploration of biological processes in live cells and *in vivo*.[13,14] Because small changes in pH_{mit} may result in a significant impact on mitochondrial biological functions, it is very important to develop ideal fluorescent probes for accurate measurement of subtle changes in pH within mitochondria. These probes should possess the following unique characteristics: (1) maximum fluorescence emission wavelengths are in the NIR region for lower interference from background fluorescence, (2) a large Stokes shift for minimizing reabsorption of emitted photons from chromophores, as well as good mitochondria-targeted capability. Although protein probes[15] and small molecule probes[16] have been reported for mitochondrial pH detection, NIR fluorescent probes with a large Stokes shift and good targeting capability are rare.

To solve these problems, we have fabricated a novel fluorescent probe, (*E*)-3-((*E*)-2-chloro-3-((*E*)-2-(1-ethyl-3,3-dimethylindolin-2-ylidene)ethylidene)cyclohex-1-enyl)-1-(4-(dimethylamino)phenyl)-prop-2-en-1-one (**Spring Red**), based on a long π-conjugated system containing a dimethylamino group (Scheme 1). The relatively long conjugated system with this structure is expected to fluoresce in the NIR region. Moreover, from existing studies, we consider that structural asymmetry of **Spring Red** may account for a large Stokes shift, ascribing to more energetically distinct ground and excited states.[17]

For the purpose of reporting alterations of mitochondrial pH, a pH-sensitive dimethylamino group is introduced to tune fluorescent properties of the scaffold. Under relatively acidic conditions, lone pair electrons of nitrogen conjugating with the π-electron system disappeared upon protonation. As a consequence, p–π conjugation fading results in gradual fluorescence decrease and blue shift of emission wavelength. In contrast to this, the fluorescent intensity of the probe should increase with the rise in pH. We confirmed that the protonation of the dimethylamino group could control fluorescence properties of **Spring Red** by molecular-orbital (DFT) calculations (Fig. S1, ESI†). Moreover, a resonance

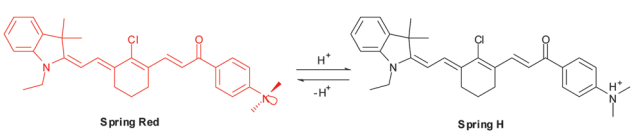

Scheme 1 Proposed mechanism for fluorescence change of **Spring Red**.

College of Chemistry, Chemical Engineering and Materials Science, Collaborative Innovation Center of Functionalized Probes for Chemical Imaging, Key Laboratory of Molecular and Nano Probes, Ministry of Education, Shandong Normal University, Jinan 250014, P. R. China. E-mail: tangb@sdnu.edu.cn; Tel: +86 531-8618-0017

† Electronic supplementary information (ESI) available: Detailed synthetic procedure and characterization data. See DOI: 10.1039/c4cc01390e

structure of **Spring Red** with a lipophilic cation (Scheme S2, ESI†) is apt to accumulate in mitochondria due to the mitochondrial membrane potential.[18] Thus, this well-designed compound is surmised to be capable of labelling alkali organelles, mitochondria, and reversibly indicating the changes in mitochondrial pH. This compound was easily prepared by facile synthesis, and characterized by UV/Vis, ^{1}H NMR, ^{13}C NMR and HRESI-MS spectroscopy (see ESI†).

The spectral properties of **Spring Red** were studied systematically. The UV/Vis absorption or excitation and emission profiles are evidenced in ESI† (Fig. S2). As expected, its emission wavelength is in the NIR region, and its Stokes shift is 150 nm. As a result, the accuracy of mitochondrial pH measurement is drastically improved, which provides an ideal high-resolution fluorescent imaging probe for organelle labelling.

Fluorescent responses of **Spring Red** toward various pH values were examined systematically in universal buffer solution (0.1 M citric acid, 0.1 M KH_2PO_4, 0.1 M $Na_2B_4O_7$, 0.1 M Tris, 0.1 M KCl),[19] in order to test the hypothesis concerning regulatory function of the dimethylamino group for fluorescence properties. As shown in Fig. 1, the pH titration results imply that **Spring Red** fluorescence is remarkably pH-dependent from pH 5.0 to 8.0 with a pK_a of 6.3, and the fluorescence intensity is greater in alkali than in acidic environments. Particularly, **Spring Red** gives a strong NIR emission peaked at 680 nm and pH ~ 8.0, and thereby it affords a useful pattern to visualize intracellular mitochondria due to an alkali environment inside mitochondria, and also indicates changes in mitochondrial pH. Further investigations demonstrate that fluorescence of **Spring Red** is basically unperturbed by relative biological components including common cations and ROS (Fig. S3, ESI†).

We next performed colocalization imaging experiments in human hepatoma cells (HepG2) to observe intracellular distribution patterns of **Spring Red**. Cultured cell lines were stained with **Spring Red** for 10 min, and then we studied uptake and internalization of the probe by live cells and mitochondria. At the same time, Mito-Tracker Green, a commercial mitochondrial dye, serves to label mitochondria in order to assess targeting mitochondria capability of **Spring Red**. Direct visual evidence suggested that **Spring Red** fluoresced brightly in HepG2 cells (Fig. 2a). From a contrasting merged image of the probe and Mito-Tracker Green staining, we found that fluorescence brightness of **Spring Red** within the cell was very heterogeneous, well overlapped with Mito-Tracker Green imaging with a colocalization coefficient of 0.91 (Fig. 2a–c). Obviously, it gives rise to brighter fluorescence in mitochondria. Further evaluation for targeting mitochondria capability of **Spring Red** was carried out in zebrafish. As shown in Fig. 2d–f, there is more extensive fluorescence in the heart region of zebrafish treated with **Spring Red**, mainly due to the high concentration of mitochondria in heart tissue.[20] In addition, the similar results were obtained from localization-imaging experiments of Mito-Tracker Green in zebrafish (Fig. S4, ESI†). Moreover, three analogues of **Spring Red** were synthesized, and colocalization-imaging experiments showed that they also accumulate in mitochondria to some extent (Fig. S5, ESI†), which indicate that the main structure of **Spring Red** plays an important role in targeting mitochondria. These results clearly suggest that **Spring Red** can diffuse fast into mitochondria and fluoresce strongly because of relatively alkali conditions in mitochondria, and is well suitable for *in vivo* imaging.

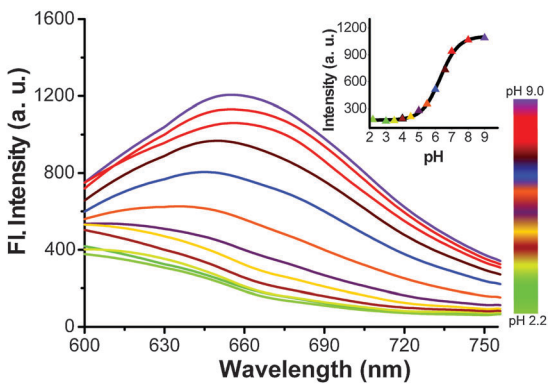

Fig. 1 Fluorescence spectral changes of **Spring Red** (30 μM) with various pH values from 2.2 to 9.0 (λ_{ex} = 530 nm, 10 mM universal buffer). Inset: sigmoidal fitting of the pH-dependent fluorescence intensity at 680 nm.

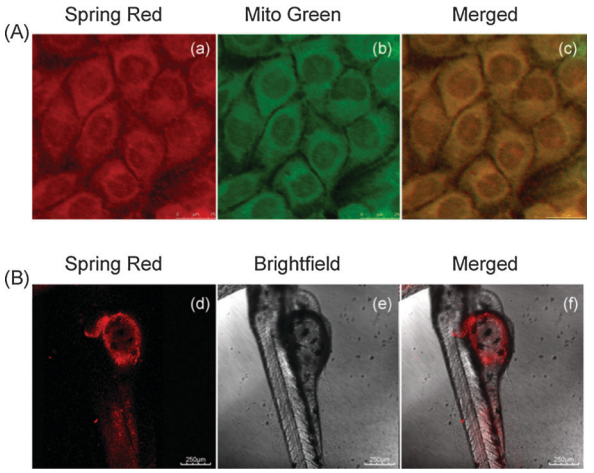

Fig. 2 Confocal fluorescence imaging of **Spring Red** in HepG2 cells (A) and zebrafish (B). (a) **Spring Red** (30 μM, λ_{ex} = 543 nm, collected in the range of 650–800 nm). (b) Mito-Tracker Green (25 nM, λ_{ex} = 488 nm, collected in the range of 495–520 nm). (c) Merged images of a and b. (d) **Spring Red** in zebrafish. (e) Brightfield image. (f) Merged images of d and e.

For studying whether the probe possesses dynamic imaging features, **Spring Red** was used to monitor intracellular pH changes. The *in situ* calibration curve for pH measurements in HepG2 cells was obtained using high K^+ buffer and ionophore nigericin[21] in bath solutions of defined pH (Fig. 3). The fluorescence intensity of **Spring Red** (Fig. 3a) inside cells enhances proportionally with an increase of pH values. The mean intensity at different pH in the cells was quantified as in Fig. 3b, showing pH-dependence over the pH range of 4.0–8.5, with the regression equation $Y = 0.3714x - 1.883$ (R^2 = 0.9958). Moreover, leakage basically did not occur over the course of imaging experiments (even 30 min) and the probe was resistant to photobleaching (Fig. S6–S8, ESI†), as well as low cell toxicity (Fig. S9, ESI†), which permit a prolonged observation time *in vivo*.

It was reported that lactate and pyruvate were exploited to cause mitochondria acidification.[15a] Under these conditions,

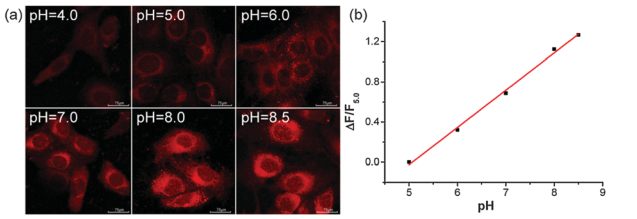

Fig. 3 (a) Fluorescent confocal microscopy images of **Spring Red** (30 μM) in HepG2 cells defined at pH 4.0–8.5. (b) Intracellular pH calibration curve of **Spring Red** in HepG2 cells from (a). $\Delta F = F - F_{5.0}$ (F: mean fluorescence intensity at different pH values; $F_{5.0}$: mean fluorescence intensity at pH = 5.0). The excitation wavelength was 543 nm and the images were collected at 650–800 nm.

fluorescence images of HepG2 cells were captured. During normal incubations, HepG2 cells exhibited a mitochondrial pH of 7.96 ± 0.13 (Fig. 4a). In the presence of glucose, pH did not change basically from the analysis of images and fluorescent intensity data output (Fig. 4b). Upon the treatment of lactate and pyruvate, steady decreases occurred in pH from 7.97 to 7.14. Subsequently, after lactate and pyruvate were removed, pH values reversed gradually to some degree from 7.14 to 7.45. The pH did not get back to the original level after washout in contrast to the previous report, probably due to slight leakage of the probe in the cells treated with lactate/pyruvate, which led to 0.51 pH unit difference to the initial level. However, the tendency of mitochondrial pH changes measured by this method is in agreement with that under similar conditions in previous reports.[15a] In addition, we applied **Spring Red** in HepG2 cells to determine the pH changes in the apoptosis process, induced by L-buthionine sulfoximine (BSO).[22] The fluorescence intensity of **Spring Red** decreased in BSO-treated cells during 1 h, indicating a decline of the pH value in cellular apoptosis (Fig. S10, ESI†).[23] All the results suggest that this fluorescent probe can real-time monitor small pH alterations inside mitochondria.

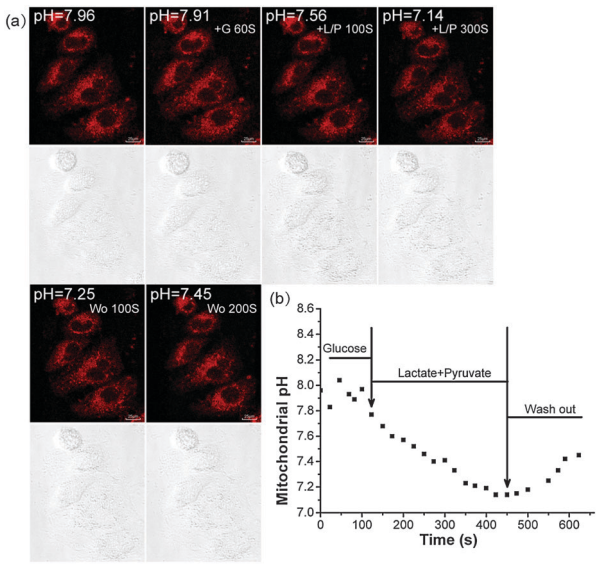

Fig. 4 (a) Confocal microscopy image of **Spring Red** (30 μM) in HepG2 cells under different conditions. (b) Effect of glucose and lactate/pyruvate perfusion on mitochondrial at different time. The excitation wavelength was 543 nm and the images were collected at 650–800 nm.

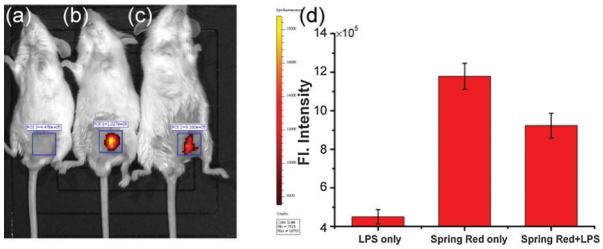

Fig. 5 Representative fluorescence images (pseudo-color) of mice injected with **Spring Red** during LPS-mediated inflammatory response *in vivo*. (a) Only LPS was injected for control. (b) Only **Spring Red** was injected. (c) LPS was injected into the peritoneal cavity of the mice, followed by injection with **Spring Red** (50 μM). (d) Quantification of fluorescence emission intensity from group a–c. Representative images of mice from replicate experiments (n = 3). The mean fluorescence intensity from the mice peritoneal cavity was output. The mice were imaged with an excitation filter (530 nm) and an emission filter (670 nm).

Finally, we investigated the application of **Spring Red** to visualize pH changes in an abdominal inflammation model induced by lipopolysaccharides (LPS).[24–26] Two mice suffered an acute inflammatory response in the peritoneal cavity *via* skin-pop injection of LPS (Fig. 5a and c). One of the mice was then injected with **Spring Red** (Fig. 5c). This mouse treated with both LPS and **Spring Red** (Fig. 5c) exhibited lower fluorescence intensity (pseudo-color) than that of only **Spring Red**-treated mouse (Fig. 5b), indicating the decrease of the pH value in the inflammatory tissues.[27–29] As a control, the mice treated with LPS but not with **Spring Red** showed almost no fluorescence (Fig. 5a). The intensity was quantified, and the data imply that the fluorescence intensity of **Spring Red** in the mice with abdominal inflammation shows an obvious decrease (Fig. 5d). Taken together, these results demonstrate that **Spring Red** is useful for *in vivo* imaging and can detect the pH changes in small animals.

In conclusion, we have presented a novel near-infrared-emitting fluorescent probe for sensing subtle pH changes with an unprecedented large Stokes shift. It also exhibits good photostability and low cytotoxicity. Fluorescence images of live cells and *in vivo* reveal that it can easily diffuse into mitochondria and reliably report pH changes under acidic conditions, cellular apoptosis or inflammation response. Overall, the merits of **Spring Red** impart a faithful estimation of small mitochondrial pH alterations in complicated biological systems, and also it has been the first NIR fluorescent emission probe for measurement of mitochondrial pH up to now. Moreover, the proposed method provides a new strategy for quantitative biology of molecular events inside other subcellular organelles.

This work was supported by the 973 Program (2013CB933800), the National Natural Science Foundation of China (21227005, 21390411, 91313302, 21035003a, 21205073) and the Program for Changjiang Scholars and Innovative Research Team in University.

References

1 Y. Yamada and H. Harashima, *Adv. Drug Delivery Rev.*, 2008, **60**, 1439–1462.
2 R. Rizzuto, D. De Stefani, A. Raffaello and C. Mammucari, *Nat. Rev. Mol. Cell Biol.*, 2012, **13**, 566–578.
3 D. C. Wallace, *Nat. Rev. Cancer*, 2012, **12**, 685–698.
4 S. Fulda, L. Galluzzi and G. Kroemer, *Nat. Rev. Drug Discovery*, 2010, **9**, 447–464.

5 B. Chance, H. Sies and A. Boveris, *Physiol. Rev.*, 1979, **59**, 527–605.
6 R. S. Balaban, S. Nemoto and T. Finkel, *Cell*, 2005, **120**, 483–495.
7 A. M. James, Y. Collins, A. Logan and M. P. Murphy, *Trends Endocrinol. Metab.*, 2012, **23**, 429–434.
8 V. Gogvadze, S. Orrenius and B. Zhivotovsky, *Apoptosis*, 2009, **14**, 624–640.
9 V. Gogvadze, S. Orrenius and B. Zhivotovsky, *Semin. Cancer Biol.*, 2009, **19**, 57–66.
10 T. Ueno and T. Nagano, *Nat. Methods*, 2011, **8**, 642–645.
11 M. Fernández-Suárez and A. Y. Ting, *Nat. Rev. Mol. Cell Biol.*, 2008, **9**, 929–943.
12 S. Chen, Y. Hong, Y. Liu, J. Liu, C. W. T. Leung, M. Li, R. T. K. Kwok, E. Zhao, J. W. Y. Lam, Y. Yu and B. Tang, *J. Am. Chem. Soc.*, 2013, **135**, 4926–4929.
13 J. V. Frangioni, *Curr. Opin. Chem. Biol.*, 2003, **7**, 626–634.
14 S. A. Hilderbrand and R. Weissleder, *Curr. Opin. Chem. Biol.*, 2010, **14**, 71–79.
15 (*a*) J. Llopis, J. M. Mccaffery, A. Miyawaki, M. G. Farquhar and R. Y. Tsien, *Proc. Natl. Acad. Sci. U. S. A.*, 1998, **95**, 6803–6808; (*b*) L. Wei-LaPierre, G. Gong, B. J. Gerstner, S. Ducreux, D. I. Yule, S. Pouvreau, X. Wang, S. S. Sheu, H. Cheng, R. T. Dirksen and W. Wang, *J. Biol. Chem.*, 2013, **288**, 10567–10577; (*c*) M. Tantama, Y. P. Hung and G. Yellen, *J. Am. Chem. Soc.*, 2011, **133**, 10034–10037.
16 (*a*) A. Takahashi, Y. Zhang, V. E. Centonze and B. Herman, *Biotechniques*, 2001, **30**, 804–815; (*b*) D. W. Jung, M. H. Davis and G. P. Brierley, *Anal. Biochem.*, 1989, **178**, 348–354.
17 J. F. Araneda, W. E. Piers, B. Heyne, M. Parvez and R. McDonaid, *Angew. Chem., Int. Ed.*, 2011, **50**, 12214–12217.
18 (*a*) L. V. Johnson, M. L. Walsh, B. J. Bockus and L. B. Chen, *J. Cell Biol.*, 1981, **88**, 526–535; (*b*) S. T. Smiley, M. Reers, C. Mottola-Hartshorn, M. Lin, A. Chen, T. W. Smith, G. D. Steele and L. B. Chen, *Proc. Natl. Acad. Sci. U. S. A.*, 1991, **88**, 3671–3675.
19 H. M. Kim, M. J. An, J. H. Hong, B. H. Jeong, O. Kwon, J. Y. Hyon, S. C. Hong, K. J. Lee and B. R. Cho, *Angew. Chem.*, 2008, **120**, 2263–2266.
20 A. T. Hoye, J. E. Davoren, P. Wipf, M. P. Fink and V. E. Kagan, *Acc. Chem. Res.*, 2008, **41**, 87–97.
21 M. H. Lee, J. H. Han, J. H. Lee, N. Park, R. Kumar, C. Kang and J. S. Kim, *Angew. Chem., Int. Ed.*, 2013, **52**, 6206–6209.
22 J. S. Armstrong, K. K. Steinauer, B. Hornung, J. M. Irish, P. Lecane, G. M. Birrell, D. M. Peehl and S. J. Knox, *Cell Death Differ.*, 2002, **9**, 252–263.
23 D. Lagadic-Gossmann, L. Huc and V. Lecureur, *Cell Death Differ.*, 2004, **11**, 953–961.
24 J. E. Parrillo, *N. Engl. J. Med.*, 1993, **328**, 1471–1477.
25 C. R. H. Raetz and C. Whitfield, *Annu. Rev. Biochem.*, 2002, **71**, 635–700.
26 M. S. Trent, C. M. Stead, A. X. Tran and J. A. Hankins, *J. Endotoxin Res.*, 2006, **12**, 205–223.
27 A. Lardner, *J. Leukocyte Biol.*, 2001, **69**, 522–530.
28 A. Punnia-Moorthy, *J. Oral Pathol. Med.*, 1987, **16**, 36–44.
29 F. Okajima, *Cell. Signalling*, 2013, **25**, 2263–2271.